PERGAMON

International Journal of Solids and Structures 36 (1999) 1781–1797

INTERNATIONAL JOURNAL OF SOLIDS and STRUCTURES

Finite thickness cracked layer bonded to viscoelastic substrate subjected to antiplane shear

R. C. Chang*

Department of Mechanical Engineering, St. John's and St. Mary's Institute of Technology, Tamsui, Taipei, Taiwan 25135, Republic of China

Received 21 May 1997; in revised form 14 February 1998

Abstract

An antiplane problem of a finite thickness cracked layer bonded to a viscoelastic substrate is considered. Complex potential function is derived via the application of the Laplace transform and a special technique of analytical continuation associated with the image method. A dislocation function is introduced to solve the boundary condition along the crack border by means of singular integral equations. Some typical viscoelastic models and its corresponding stress intensity factors are also discussed. The results show that, subjected to constant load, the time-dependent stress intensity factor may increase or decrease with time evolution. This is affected by the orientation of crack as well as the relative strength of the layer and substrate.

1. Introduction

The purpose of this work is to investigate a finite thickness cracked layer bonded to a viscoelastic half-space substrate subjected to antiplane shear. Most engineering materials, including metals, are known to creep under sustained constant loads and relax while being subjected to a constant strain. The failure mechanism is mainly dependent on the relative strength of the cohesive layer and the substrate. The understanding and prediction of the long-term failure behavior is important because products with time-dependent properties have been widely applied in many engineering designs.

For viscoelastic fracture, Schapery (1984) showed that the parameters analogous to the J integral and energy release rate may be used for quasi-static crack growth in a class of nonlinear viscoelastic materials under finite strain. Schapery also developed the correspondence principles which establish a simple relationship between mechanical states of elastic and viscoelastic media. When viscoelastic effects are included in the analysis, it seems that analytic results may be obtained only for mode

* Fax: 00 886 2 6209832; e-mail: rcc@mail.sjsmit.edu.tw

0020–7683/99/$ - see front matter
PII: S0020–7683(98)00058–4

III deformation. Several papers have appeared in the literature dealing with crack propagation along the interface between two viscoelastic media. Sills and Benveniste (1981) determined the stress intensity factor for crack propagating steadily between two different viscoelastic half-planes, modeled as Maxwell materials, and driven by an exponentially decaying load applied to the crack surface. Banks-Sills and Benveniste (1983) considered the same problem with the materials modeled as standard solids. Atkinson and Chen (1996) found the solution of viscoelastic composite under mode III load. They considered that medium 2 is contained in a layer sandwiched between semi-infinite half space of medium 1. That is, sandwiched layer composed of two dissimilar media is derived in their work. In this paper, the multi-layers problem of three dissimilar media, even one of them may be assumed to be empty, is presented.

Honien et al. (1992) derived the solution for two circular cylindrical elastic inclusions perfectly bonded to an elastic matrix of infinite extent. They obtained a rapidly convergent series with an explicit general term involving the complex potential of the corresponding homogeneous problem via iterations of Möbius transformations. For the cracked layer, however, it is impossible to achieve a closed form solution. An alternative method for solving such complicated crack problems may be formulated in terms of a system of singular integral equations by using the related Green's function, such as dislocation or concentrated force solution, in conjunction with the technique of superposition. This method has clear advantages in solving the problem by applying a numerical treatment. In the derivation of singular integral equations, the selection of the auxiliary function determines whether the kernels have weak or strong singularities. The kernel with Cauchy-type singularity has been widely used to solve many crack problems which can be reduced to a system of algebraic equations. The numerical results are obtained by applying appropriate orthogonal polynomials. On the other hand, the singular integral equation with a logarithmic singular kernel is also applied frequently to crack problems. Chen and Cheung (1990) solved some elastic half-plane problems by using log-type singular integral equations based on elementary solutions and the principle of superposition. Recently, Chao and Gao (1997) solved the thin cracked layer bonded to an elastic half-space media problem using iterations of Möbius transformations and singular integral technique.

In this work, a viscoelastic problem is derived by using the Laplace transform, and the multiple layers solution is found by the image method, also called iterations of Möbius transformations. The application of the log-type singular integral technique is used for solving the cracked body. Some typical examples are obtained by a Kelvin–Maxwell three parameters model to simulate the viscoelastic property. The result for the time-dependent stress intensity factor is also discussed.

2. Governing equation

The relation between strains ε_{ij} and stresses σ_{ij} can be written in the form

$$\varepsilon_{ij} = s_{ijkl}\sigma_{kl} \quad (i, j, k, l = 1, 2, 3), \tag{1}$$

where s_{ijkl} denote the compliance tensors. Unless otherwise stated, repeated indices imply summation. Due to the symmetry of material property, the generalized Hooke's law shown in eqn (1) can be expressed in contracted notation as

$$\varepsilon_m = s_{mn}\sigma_n \quad (m, n = 1, 2, \ldots, 6) \tag{2}$$

where the standard correspondence is adopted, that is

$$\{\varepsilon_m\} = [\varepsilon_{11}, \varepsilon_{22}, \varepsilon_{33}, 2\varepsilon_{23}, 2\varepsilon_{31}, 2\varepsilon_{12}]^T,$$
$$\{\sigma_m\} = [\sigma_{11}, \sigma_{22}, \sigma_{33}, \sigma_{23}, \sigma_{31}, \sigma_{12}]^T, \tag{3}$$

and the superscript T denotes the transpose. The relation between s_{mn} and s_{ijkl} is analogous except that the numerical factors are needed, e.g. $s_{11} = s_{1111}$, $s_{14} = 2s_{1123}$, $s_{44} = 4s_{2323}, \ldots$, etc. For two-dimensional problem, i.e., with geometry and external loading invariant in the direction normal to x_1x_2-plane, all physical components are independent of the coordinate x_3. Furthermore, a material body is said to undergo anti-plane deformation when the displacement field satisfies

$$u_1 = u_2 = 0, \quad u_3 = u_3(x_1, x_2), \tag{4}$$

i.e., the only nonvanishing component of displacement, with respect to a Cartesian coordinate system $0x_1x_2x_3$, is u_3, which is a function of the coordinates x_1 and x_2 only. The only nonvanishing infinitesimal strain components are

$$\varepsilon_{31} = \varepsilon_{13} = \tfrac{1}{2}u_{3,1},$$
$$\varepsilon_{32} = \varepsilon_{23} = \tfrac{1}{2}u_{3,2}, \tag{5}$$

where a subscript after a comma stands for differentiation with respect to this index, i.e. $A_{i,j} = \partial A_i/\partial x_j$. The equation of equilibrium without body forces can be written as

$$\sigma_{31,1} + \sigma_{32,2} = 0. \tag{6}$$

According to the solution given by Lekhnitskii (1963), the complex variable z can be defined as

$$z = x_1 + \mu x_2, \tag{7}$$

where μ is the root of the characteristic equation

$$s_{44} - 2s_{45}\mu + s_{55}\mu^2 = 0, \tag{8}$$

with positive imaginary part. Therefore, the stresses and displacement can be expressed by a holomorphic function $\phi(z)$ as

$$\sigma_{31} = 2\Re\{\mu\phi'(z)\},$$
$$\sigma_{32} = -2\Re\{\phi'(z)\},$$
$$u_3 = 2\Re\{ic\phi(z)\}, \tag{9}$$

where $\Re$ indicates the real part of a complex and

$$c = (s_{44}s_{55} - s_{45}^2)^{1/2}. \tag{10}$$

Similarly, the resultant torque becomes

$$T = \int[\sigma_{31}\,dx_2 - \sigma_{32}\,dx_1] = 2\Re\{\phi(z)\} + \Gamma_0, \tag{11}$$

where Γ_0 denotes the torsion at an arbitrary point. Equation (9) and (11) give the complex potential expression for an anisotropic elastic material. For viscoelastic material, the time dependent strains ε_{ij} and stresses σ_{ij} can be written in the hereditary integral form (Flügge, 1975)

$$\varepsilon_{ij}(t) = s_{ijkl}(0)\sigma_{kl}(t) + \int_0^t s'_{ijkl}(t-\xi)\sigma_{kl}(\xi)\,\mathrm{d}\xi \quad (i,j,k,l = 1,2,3), \tag{12}$$

where $s_{ijkl}(t)$ denote the creep compliance tensors. In contracted notation, eqn (12) can be expressed as

$$\varepsilon_m = S_{mn} * \sigma_n \quad (m,n = 1,2,\ldots,6). \tag{13}$$

The quantities S_{mn} are the linear integral operators, applied to the function $g(t)$

$$S_{mn} * g(t) = s_{mn}(0)g(t) + \int_0^t s'_{mn}(t-\xi)g(\xi)\,\mathrm{d}\xi. \tag{14}$$

Taking the Laplace transform, eqn (13) becomes

$$\hat{\varepsilon}_m(p) = \hat{s}_{mn}(p)\hat{\sigma}_n(p), \tag{15}$$

where the notation $\hat{f}(p)$ denotes the Laplace transform of $f(t)$ and p is the Laplace variable. Consequently, following the Lekhnitskii's expression, the stresses and displacement of viscoelastic field can be written as

$$\begin{aligned}
\hat{\sigma}_{31} &= 2\Re\{\hat{\mu}\hat{\phi}'(\hat{z})\},\\
\hat{\sigma}_{32} &= -2\Re\{\hat{\phi}(\hat{z})\},\\
\hat{u}_3 &= 2\Re\{i\hat{c}\hat{\phi}(\hat{z})\},\\
\hat{T} &= 2\Re\{\hat{\phi}(\hat{z})\} + \hat{\Gamma}_0,
\end{aligned} \tag{16}$$

where

$$\begin{aligned}
\hat{c} &= (\hat{s}_{44}\hat{s}_{55} - \hat{s}_{45}^2)^{1/2},\\
\hat{z} &= x_1 + \hat{\mu}x_2,
\end{aligned} \tag{17}$$

and $\hat{\mu}$ is the root with positive imaginary part of the characteristic equation

$$\hat{s}_{44} - 2\hat{s}_{45}\hat{\mu} + \hat{s}_{55}\hat{\mu}^2 = 0. \tag{18}$$

To simplify the problem, only isotropic materials are considered in the following discussion. Notes that the anisotropic formulation of anti-plane problem in the present derivation is still valid for an isotropic body. For isotropic material, $\hat{s}_{44} = \hat{s}_{55} = \hat{s}$, $\hat{s}_{45} = 0$, eqn (17) becomes

$$\hat{c} = (\hat{s}_{44}\hat{s}_{55} - \hat{s}_{45}^2)^{1/2} = \hat{s}, \tag{19}$$

then the isotropic stresses and displacement are given by

$$\begin{aligned}
\hat{\sigma}_{31} &= 2\Re\{i\hat{\phi}'(z)\},\\
\hat{\sigma}_{32} &= -2\Re\{\hat{\phi}'(z)\},\\
\hat{u}_3 &= 2\Re\{i\hat{s}\hat{\phi}(z)\},
\end{aligned}$$

$$\hat{T} = 2\Re\{\hat{\phi}(z)\} + \hat{\Gamma}_0, \tag{20}$$

where $z = \hat{z}$ because the characteristic value μ is independent on time in isotropic case, i.e., $\mu = \hat{\mu} = i$.

3. Bilinear transformation

The purpose of this section is to show briefly, for the homogeneous problem, how the solution of multiple layer problems can be obtained by simple algebraic manipulations. First, consider the double layer problem as shown in Fig. 1. The upper and lower half space are occupied by D_1 and D_2, respectively. The upper half space (D_1) is subjected to arbitrary singularities. Assume that $\hat{\phi}_0(z)$ represents these singularities as if D_1 occupied the whole space. $\hat{\psi}_1(z)$ and $\hat{\psi}_2(z)$ are the corresponding holomorphic functions in the regions D_1 and D_2. Therefore, the complex potential is given by

$$\begin{aligned} \hat{\phi}_1(z) &= \hat{\phi}_0(z) + \hat{\psi}_1(z), \quad z \in D_1, \\ \hat{\phi}_2(z) &= \hat{\psi}_2(z), \quad z \in D_2. \end{aligned} \tag{21}$$

Assuming that the interface has perfect bonding, the traction (or resultant force) and displacement across the interface must be continuous. Therefore,

$$\hat{T}^{+} + \hat{T}^{-}, \quad \hat{u}_3^{+} = \hat{u}_3^{-}, \tag{22}$$

along x_1-axis, where superscript + and − refer to upper and lower half-space, respectively. Using eqn (20), eqn (22) can be written as

$$i\hat{s}_1[\hat{\phi}_0(x_1) + \hat{\psi}_1(x_1)] - i\hat{s}_1[\bar{\hat{\phi}}_0(x_1) + \bar{\hat{\psi}}_1(x_1)] = i\hat{s}_2[\hat{\psi}_2(x_1) - \bar{\hat{\psi}}_2(x_1)], \tag{23}$$

$$[\hat{\phi}_0(x_1) + \hat{\psi}_1(x_1)] + [\bar{\hat{\phi}}_0(x_1) + \bar{\hat{\psi}}_1(x_1)] = \hat{\psi}_2(x_1) + \bar{\hat{\psi}}_2(x_1). \tag{24}$$

One of the important properties of holomorphic functions used in the method of analytical continuation is that if $\psi(z)$ is holomorphic in upper half space (or lower half space), then $\bar{\psi}(z)$ is holomorphic in lower half space (or upper half space). From this property, the holomorphic function of the half space can be extended to the whole space. Holomorphic functions $\hat{\psi}_1(z)$ and $\hat{\psi}_2(z)$ in eqn (21) need to satisfy continuity of torsion and displacement along the interface x_1-axis. Substituting eqn (21) into eqns (9) and (11), after simple algebraic manipulations, it gives

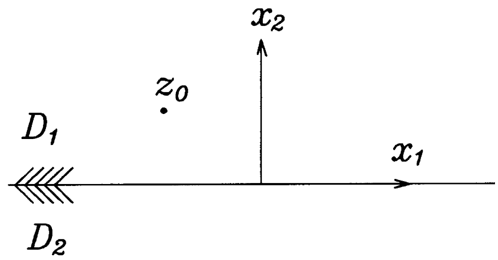

Fig. 1. Double-layers with singularities at upper layer.

$$\hat{\phi}_1(z) = \hat{\phi}_0(z) + \hat{\alpha}\bar{\hat{\phi}}_0(z), \quad z \in D_1,$$
$$\hat{\phi}_2(z) = (1+\hat{\alpha})\hat{\phi}_0(z), \quad z \in D_2, \tag{25}$$

where overbar denotes the complex conjugate, and α is a bi-material constant defined as

$$\hat{\alpha} = \frac{\hat{s}_1 - \hat{s}_2}{\hat{s}_1 + \hat{s}_2} \tag{26}$$

which $\hat{s}$ is defined in eqn (19). The subscript value denote dissimilar media D_1 and D_2. Equation (25) is the solution for dissimilar media subjected to arbitrary singularities. Referring to Fig. 2, consider a thin layer with thickness $2h$ bonded to two different media. The notations D, D_1 and D_2 denote the middle thin layer, upper and lower region, respectively. Following eqn (25), the solution for the triple-layers can be solved by the method of image (Honein et al., 1992; Chao and Gao, 1997). The stress functions satisfying the continuous conditions on L_1 are given by

$$\hat{\phi}_1(z) = \hat{\phi}_0(z) + \hat{\alpha}_1\hat{\phi}_0(z), \quad z \in D_1,$$
$$\hat{\phi}_2(z) = \hat{\phi}_0(z) + \hat{\alpha}_1\overline{\hat{\phi}_0(A_1 z)}, \quad z \in D_2,$$
$$\hat{\phi}(z) = \hat{\phi}_0(z) - \hat{\alpha}_1\overline{\hat{\phi}_0(A_1 z)}, \quad z \in D, \tag{27}$$

with

$$\hat{\alpha}_1 = \frac{\hat{s} - \hat{s}_1}{\hat{s} + \hat{s}_1}, \tag{28}$$

where $\hat{\phi}_0(z)$ is the singularities at D and the transform function is defined as $A_1 z = \bar{z} + 2hi$. Another mapping function $A_2 z = \bar{z} - 2hi$ is used to deal with the continuous conditions along L_2, and eqn (27) becomes

$$\hat{\phi}_1(z) = \hat{\phi}_0(z) + \hat{\alpha}_1\hat{\phi}_0(z) + \hat{\alpha}_2\overline{\hat{\phi}_0(A_2 z)} + \hat{\alpha}_1\hat{\alpha}_2\hat{\phi}_0(A_1 A_2 z), \quad z \in D_1,$$
$$\hat{\phi}_2(z) = \hat{\phi}_0(z) + \hat{\alpha}_1\overline{\hat{\phi}_0(A_1 z)} + \hat{\alpha}_2\hat{\phi}_0(z) + \hat{\alpha}_1\hat{\alpha}_2\overline{\hat{\phi}_1(A_1 z)}, \quad z \in D_2,$$
$$\hat{\phi}(z) = \hat{\phi}_0(z) + \hat{\alpha}_1\overline{\hat{\phi}_1(A_1 z)} + \hat{\alpha}_2\overline{\hat{\phi}_0(A_2 z)} + \hat{\alpha}_1\hat{\alpha}_2\hat{\phi}_0(A_1 A_2 z), \quad z \in D, \tag{29}$$

with

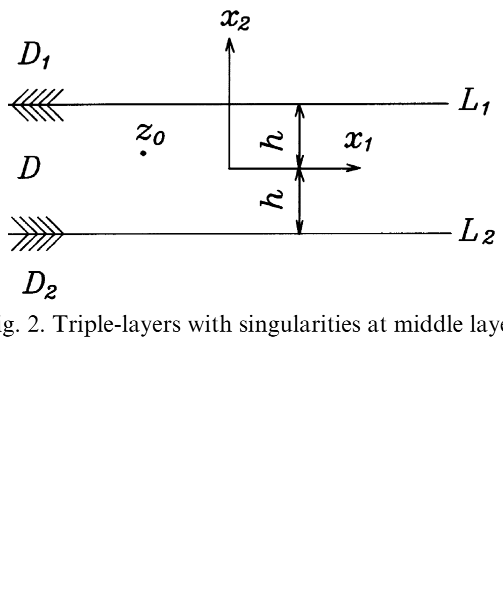

Fig. 2. Triple-layers with singularities at middle layer.

$$\hat{\alpha}_2 = \frac{\hat{s}-\hat{s}_2}{\hat{s}+\hat{s}_2}. \tag{30}$$

Repeating eqn (27) and eqn (29), the stress functions are given by

$$\hat{\phi}(z) = \hat{\phi}_0 + \sum_{n=1}^{\infty}(\hat{\alpha}_1\hat{\alpha}_2)^n\hat{\phi}_0(M^n z) + \sum_{n=1}^{\infty}(\hat{\alpha}_1\hat{\alpha}_2)^n\hat{\phi}_0(N^n z) + \hat{\alpha}_1\sum_{n=0}^{\infty}(\hat{\alpha}_1\hat{\alpha}_2)^n\overline{\hat{\phi}_0(A_1 N^n z)}$$
$$+\hat{\alpha}_2\sum_{n=0}^{\infty}(\hat{\alpha}_1\alpha_2)^n\overline{\hat{\phi}_0(A_2 M^n z)}, \quad z\in D, \tag{31}$$

$$\hat{\phi}_1(z) = (1+\hat{\alpha}_1)\left\{\hat{\phi}_0(z)+\hat{\alpha}_2\sum_{n=1}^{\infty}(\hat{\alpha}_1\hat{\alpha}_2)^n\overline{\hat{\phi}_0(A_2 M^n z)}+\sum_{n=0}^{\infty}(\hat{\alpha}_1\hat{\alpha}_2)^n\hat{\phi}_0(M^n z)\right\}, \quad z\in D_1, \tag{32}$$

$$\hat{\phi}_2(z) = (1+\hat{\alpha}_2)\left\{\hat{\phi}_0(z)+\hat{\alpha}_1\sum_{n=1}^{\infty}(\hat{\alpha}_1\hat{\alpha}_2)^n\overline{\hat{\phi}_0(A_1 N^n z)}+\sum_{n=0}^{\infty}(\hat{\alpha}_1\hat{\alpha}_2)^n\hat{\phi}_0(N^n z)\right\}, \quad z\in D_2, \tag{33}$$

where

$$A_k z = \bar{z}-(-1)^k 2ih \quad (k=1,2), \tag{34}$$

and $M^n z = (A_1A_2)^n z = z+4nih$, $N^n z = (A_2A_1)^n z = z-4nih$, which is called Möbius transformation or Bilinear transformation (Saff and Snider, 1976). Equations (31)–(33) are uniformly convergent since the material constants provide $|\alpha_1\alpha_2| < 1$ (Honein et al. 1992). Taking the inverse Laplace transform of eqns (31)–(33), the viscoelastic solution to multiple layers is found.

Consider a thin layer bonded to a half-space substrate, as shown in Fig. 3. In terms of previous derivative, this means the upper half-space is empty. Equations (23)–(26) yield $\hat{\alpha}_1 = 1$ or -1 if the boundary condition of L_1 is displacement or traction specified, respectively. This implies that $\hat{s}_1 = 0$ as $\hat{\alpha}_1 = 1$, and $\hat{s}_1$ tends to infinite as $\hat{\alpha}_1 = -1$. Even for these conditions, the complex potential solution derived in eqns (31)–(33) still leads to a convergent series, which can be obtained by differentiating the formal series solution term by term. Substituting $\hat{\alpha}_1 = -1$ into eqns (31)–(33) gives

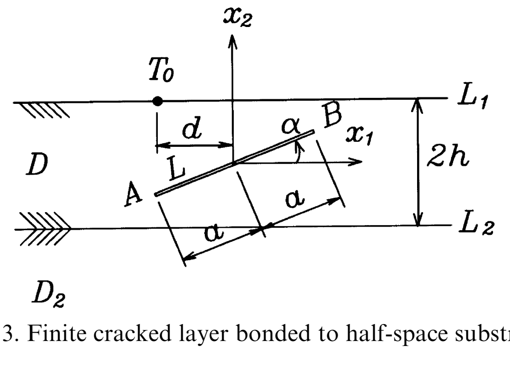

Fig. 3. Finite cracked layer bonded to half-space substrate.

$$\hat{\phi}(z) = \hat{\phi}_0(z) + \sum_{n=1}^{\infty}(-1)^n\hat{\alpha}_2^n\hat{\phi}_0(M^n z) + \sum_{n=1}^{\infty}(-1)^n\hat{\alpha}_2^n\hat{\phi}_0(N^n z) + \sum_{n=0}^{\infty}(-1)^{n+1}\hat{\alpha}_2^n\overline{\hat{\phi}_0(A_1 N^n z)}$$

$$+ \sum_{n=0}^{\infty}(-1)^n\hat{\alpha}_2^{n+1}\overline{\hat{\phi}_0(A_2 M^n z)}, \quad z \in D, \quad (35)$$

$$\hat{\phi}_2(z) = (1+\hat{\alpha}_2)\left\{\hat{\phi}_0(z) + \sum_{n=1}^{\infty}(-1)^{n+1}\hat{\alpha}_2^n\overline{\hat{\phi}_0(A_1 N^n z)} + \sum_{n=0}^{\infty}(-1)^n\hat{\alpha}_2^n\hat{\phi}_0(N^n z)\right\}, \quad z \in D_2, \quad (36)$$

where $\hat{\phi}_1(z)$ vanishes for this case. Equation (35) and (36) are the solution to a thin layer bonded to another substrate with traction free condition on the surface.

4. Finite thickness cracked layer

A $2h$ thickness layer bonded to a half-space substrate subjected to an antiplane shear T_0 on the layer surface is considered (Fig. 3). The crack has length $2a$ and arbitrary angle α. This problem can be solved by using the superposition method associated with the application of singular integral technique. The singular function of homogeneous medium corresponding to a point force T_0 applied at z_0 is given by

$$\phi_0^{(1)}(z) = \frac{iT_0}{4\pi}\log(z-z_0)H(t-t_0), \quad (37)$$

where $H(t-t_0)$ denotes the Heaviside unit step function. Therefore, taking the Laplace transform to eqn (37) and substituting it into eqns (35) and (36), gives

$$\hat{\phi}^{(1)}(z) = \frac{iT_0\, e^{-t_0 p}}{4\pi p}\left[\log(z-z_0) + \sum_{n=1}^{\infty}(-1)^n\hat{\alpha}_2^n\log(z+4nhi-z_0)\right.$$

$$+ \sum_{n=1}^{\infty}(-1)^n\hat{\alpha}_2^n\log(z-4nhi-z_0) + \sum_{n=0}^{\infty}(-1)^{n+1}\hat{\alpha}_2^n\log(z-4nhi-2hi-\bar{z}_0)$$

$$\left.+ \sum_{n=0}^{\infty}(-1)^n\hat{\alpha}_2^{n+1}\log(z-4nhi+2hi-\bar{z}_0)\right], \quad z \in D, \quad (38)$$

$$\hat{\phi}_2^{(1)}(z) = \frac{iT_0\, e^{-t_0 p}}{4\pi p}(1+\hat{\alpha}_2)\left[\log(z-z_0) + \sum_{n=0}^{\infty}(-1)^{n+1}\hat{\alpha}_2^n\log(z-4nhi-2hi-\bar{z}_0)\right.$$

$$\left.+ \sum_{n=0}^{\infty}(-1)^n\hat{\alpha}_2^n\log(z-4nhi-z_0)\right], \quad z \in D_2. \quad (39)$$

Taking inverse Laplace transform

$$\phi^{(1)} = \int_{a_0-i\infty}^{a_0+i\infty}\hat{\phi}^{(1)}(z)\, e^{tp}\,\mathrm{d}p, \quad \phi_2^{(1)}(z) = \int_{a_0-i\infty}^{a_0+i\infty}\hat{\phi}_2^{(1)}(z)\, e^{tp}\,\mathrm{d}p, \quad (40)$$

yields the stress functions. Consider the crack L to be situated in middle layer, D, as shown in Fig. 3. The corresponding singular function of homogeneous medium is given by

$$\phi_0^{(2)}(z) = \frac{-1}{4\pi s}\int_L b(\eta)\log(z-\xi)\,d\eta, \quad \xi\in L, \tag{41}$$

where the dislocation function $b(\eta)$ indicates the component of displacement discontinuties across the dislocation line. Taking Laplace transform of eqn (41) and substituting it into eqn (31), gives

$$\begin{aligned}\hat{\phi}^{(2)}(z) = \frac{-1}{4\pi\hat{s}}\Bigg[&\int_L b(\eta)\log(z-\xi)\,d\eta + \sum_{n=1}^{\infty}(-1)^n\hat{\alpha}_2^n\int_L b(\eta)\log(z+4nhi-\xi)\,d\eta \\ &+\sum_{n=1}^{\infty}(-1)^n\hat{\alpha}_2^n\int_L b(\eta)\log(z-4nhi-\xi)\,d\eta \\ &+\sum_{n=0}^{\infty}(-1)^{n+1}\hat{\alpha}_2^n\int_L b(\eta)\log(z-4nhi-2hi-\bar{\xi})\,d\eta \\ &+\sum_{n=0}^{\infty}(-1)^n\hat{\alpha}_2^{n+1}\int_L b(\eta)\log(z-4nhi+2hi-\bar{\xi})\,d\eta\Bigg], \quad z\in D,\end{aligned} \tag{42}$$

$$\begin{aligned}\hat{\phi}_2^{(2)}(z) = \frac{-1}{4\pi\hat{s}}(1+\hat{\alpha}_2)\Bigg[&\int_L b(\eta)\log(z-\xi)\,d\eta + \sum_{n=0}^{\infty}(-1)^{n+1}\hat{\alpha}_2^n\int_L b(\eta)\log(z-4nhi-2hi-\bar{\xi})\,d\eta \\ &+\sum_{n=0}^{\infty}(-1)^n\hat{\alpha}_2^n\int_L b(\eta)\log(z-4nhi-\xi)\,d\eta\Bigg], \quad z\in D_2.\end{aligned} \tag{43}$$

Similarly, the stress functions can be solved by taking inverse Laplace transform

$$\phi^{(2)}(z) = \int_{a_0-i\infty}^{a_0+i\infty}\hat{\phi}^{(2)}(z)\,e^{tp}\,dp, \quad \phi_2^{(2)}(z) = \int_{a_0-i\infty}^{a_0+i\infty}\hat{\phi}_2^{(2)}(z)\,e^{tp}\,dp. \tag{44}$$

The unknown dislocation function $b(\eta)$ appearing in eqn (41) will be obtained on the basis that the resultant force applied on crack surface must vanish, i.e.

$$T^{(1)}(z_s)+T^{(2)}(z_s) = 0, \quad z_s\in L, \tag{45}$$

where the resultant torsion T is in eqn (11) and superscripts (1), (2) denote the resultant torsion induced by concentrated load and crack dislocation, respectively. Furthermore, the dislocation function needs to satisfy the requirement for a single-valued displacements, is

$$\int_L b(\eta)\,d\eta = 0. \tag{46}$$

5. Time-dependent stress intensity factor

In order to perform the numerical calculation, boundary conditions and material properties need to be specified. The cracked coating layer is considered as an elastic material. Without the

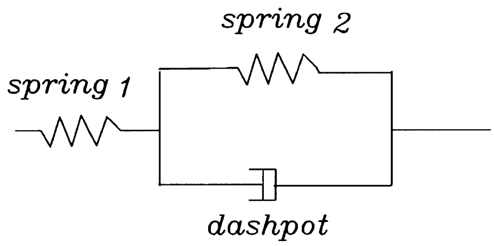

Fig. 4. Kelvin–Maxwell three parameters model.

Laplace transform, eqns (35) and (36) can also be degenerated into elastic solution. Let its material properties be

$$s_{44} = s_{55} = s_0, \quad s_{45} = 0, \quad z \in D, \tag{47}$$

where s_0 corresponds to the inverse of shear modulus. The half-space substrate D_2 is considered as a viscoelastic medium. A Kelvin–Maxwell three-parameter model is applied to simulate this viscoelastic behavior (Fig. 4). The constitutive relation shown in eqn (12) can be written as

$$\varepsilon_m(t) = s^0_{mn}\left[\sigma_n(t) + B\int_0^t f(t-\xi)\sigma_n(\xi)\,\mathrm{d}\xi\right], \tag{48}$$

where $s^0_{m,n}$ is the creep compliance at $t = 0$, and $f(t) = e^{-\lambda t}$, where λ denotes the relaxation time. B is a constant defined as $B = \lambda(s^{\infty}_{mn} - s^0_{mn})/s^0_{mn}$, where s^{∞}_{mn} is the long-term creep compliance at $t = \infty$. Meanwhile, the viscoelastic constants of D_2 are specified as

$$s^0_{44} = s^0_{55} = s^0_v, \quad s^{\infty}_{44} = s^{\infty}_{55} = s^f_v, \quad s^0_{45} = s^{\infty}_{45} = 0, \quad z \in D. \tag{49}$$

Figure 5 illustrates some creep compliance behavior for various relaxation constant $\lambda = 0.1$, 1, 10, respectively, with $s^0_v = s_0$, $s^f_v = 2s^0_v$ under constant stress σ_0. Figure 5 shows that the strain $\varepsilon(t)$

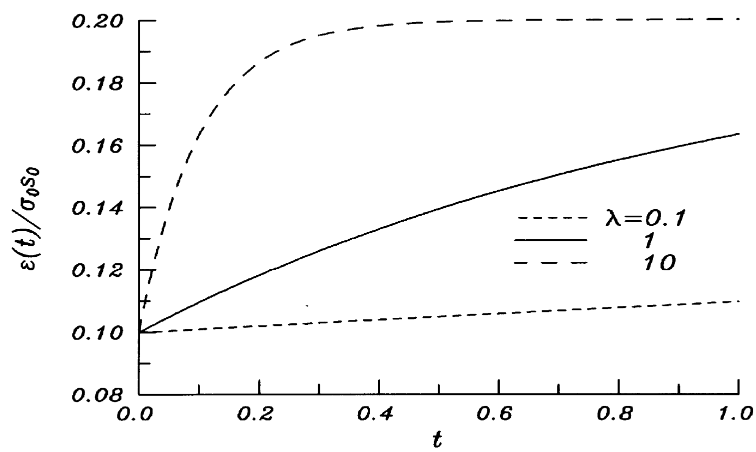

Fig. 5. Creep compliance behavior.

converges to its long-term value as $t \to \infty$. Moreover, $\varepsilon(t)$ approaches $\varepsilon(\infty)$ rapidly as λ increases. Substituting eqns (47), (49) into eqns (38), (39), the stress functions for concentrated torsion T_0 at z_0 become

$$\hat{\phi}^{(1)}(z) = \frac{iT_0\, e^{-t_0 p}}{4\pi p}[\log(z-z_0)+\log(z-2hi-\bar{z}_0) - \hat{\alpha}_2 \log(z+2hi-\bar{z}_0) - \hat{\alpha}_2 \log(z-4hi-z_0)+\cdots] \quad z \in D, \tag{50}$$

$$\hat{\phi}_2^{(1)}(z) = \frac{iT_0\, e^{-t_0 p}}{4\pi p}[\log(z-z_0)+\log(z-2hi-\bar{z}_0) + \hat{\alpha}_2 \log(z-z_0) + \hat{\alpha}_2 \log(z-2hi-\bar{z}_0)+\cdots] \quad z \in D_2, \tag{51}$$

where $\hat{\alpha}_2$ is a function of Laplace argument p. Substituting eqn (30) into eqns (50), (51) and taking the inverse Laplace transform, as an example, gives

$$\phi^{(1)}(z) = \frac{iT_0 H(t-t_0)}{4\pi}\left\{\log(z-z_0)+\log(z-2hi-\bar{z}_0) - \left[-\frac{1}{3}+\frac{1}{3}e^{-3\lambda(t-t_0)/2}\right]\log(z+2hi-\bar{z}_0) - \left[-\frac{1}{3}+\frac{1}{3}e^{-3\lambda(t-t_0)/2}\right]\log(z-4hi-z_0)+\cdots\right\}, \quad z \in D, \tag{52}$$

$$\phi_2^{(1)}(z) = \frac{iT_0 (t-t_0)}{4\pi}\left\{\log(z-z_0)+\log(z-2hi-\bar{z}_0) + \left[-\frac{1}{3}+\frac{1}{3}e^{-3\lambda(t-t_0)/2}\right]\log(z-z_0) + \left[-\frac{1}{3}+\frac{1}{3}e^{-3\lambda(t-t_0)/2}\right]\log(z-2hi-\bar{z}_0)+\cdots\right\}, \quad z \in D_2, \tag{53}$$

where $s_v^0 = s_0$, $s_v^f = 2s_v^0$. Considering crack problem, the dislocation function appearing in the singular integral of eqn (41) will be solved numerically using the appropriate interpolation formulae. In order to perform the numerical calculation, the crack is approximated by n line segments. Since the dislocation function $b(\eta)$ contains square-root singularity at the vicinity of the crack tip, the interpolation formulae in local coordinates η_1 and η_n for each crack tip element are defined as (Chen and Cheung, 1990)

$$b(\eta_1) = b_0\left(\sqrt{\frac{2d_1}{d_1+\eta_1}}-1\right)+b_1\left(\frac{d_1+\eta_1}{2d_1}\right), \tag{54}$$

and

$$b(\eta_n) = b_n\left(\sqrt{\frac{2d_n}{d_n-\eta_n}}-1\right)+b_{n-1}\left(\frac{d_n-\eta_n}{2d_n}\right), \tag{55}$$

where the dislocation function contains square-root singularity as $\eta_1 \to -d_1$ and $\eta_n \to d_n$. The interpolation formulae for the intermediate segments in local coordinates n_j $(2 \leqslant j \leqslant n-1)$ are taken as

$$b(\eta_j) = b_{j-1}\frac{d_j-\eta_j}{2d_j}+b_j\frac{d_j+\eta_j}{2d_j}, \tag{56}$$

where d_j denotes the half length of each line segment and b_j are the unknown coefficients to be determined. The traction-free condition of eqn (45), after letting z_s be the nodes of each line segment, provides $n+1$ algebraic equations. These $n+1$ integral equation together with the single-value displacement condition of eqn (46) can be solved to yield $n+2$ algebraic equation in $n+2$ unknowns, $b_0, b_1, \ldots, b_n$ and Γ_0 of eqn (11). The Mode III stress intensity factor K_{III} is defined as (Irwin, 1957)

$$K_{\mathrm{III}} = \lim_{r\to 0}\sqrt{2\pi r}\sigma_{32}(r), \tag{57}$$

where r is the radial position ahead of the crack tip. Similarly,

$$K_{\mathrm{III}} = \lim_{r\to 0}\frac{\sqrt{2\pi}}{4s\sqrt{r}}\mathrm{d}_3(r), \tag{58}$$

with r behind the crack tip. Note that $d_3(r)$ indicates the displacement jump, i.e., $d_3 = u_3^+ - u_3^-$. Therefore, from eqns (41), (54), (55) and (58), the viscoelastic stress intensity factor at two crack tips are directly related to the coefficients b_0 and b_n by (Chen and Cheung, 1990)

$$K_{\mathrm{III}} = \frac{1}{s}\sqrt{\pi d_1}b_0 \quad \text{at crack tip A,}$$

$$K_{\mathrm{III}} = \frac{1}{s}\sqrt{\pi d_n}b_n \quad \text{at crack tip B,} \tag{59}$$

where A and B denote crack tip points at left and right ends, respectively. It must be emphasized that the stress intensity factors defined in eqn (59) are time-dependent parameters.

6. Numerical results

Results of stress intensity factor for some typical examples are shown. The time-dependent stress intensity factor is expressed as dimensionless form, i.e., $K_{\mathrm{III}}/T_0a^{-1/2}$. For all cases, the geometry is $h/a = 2$, $d = 0$, and the instant of the force applies at $t_0 = 0$. Furthermore, the relative material strength $s_v^0 = s_0$, $s_v^f = 2s_v^0$ is assumed. Figure 6 illustrates the dimensionless time-dependent stress intensity factors of the horizontal crack tip-B with respect to $\lambda = 0.1$, 1, 10. It shows that, K_{III} increases monotonically with time until it reaches a constant value which is known as elastic solution. For different relaxation constant λ, K_{III} converges more rapidly as λ increases. Figure 7 shows K_{III} in the same condition except that the crack is oblique at $\alpha = 45^\circ$. In contrast with Fig. 6, the time evolution of K_{III} in this case decreases monotonically as time increases. It implies that the maximum K_{III} occurs at the instant that the external force is applied and it reduces to the elastic value while the applied force remains constant.

Figure 8 (crack tip-B) and Fig. 9 (crack tip-A) show the time-dependent K_{III} with respect to various crack angle for $\lambda = 1$. In Fig. 8, it is seen that $\alpha = 45^\circ$ has maximum value, and $K_{\mathrm{III}} = 0$ at $\alpha = 90^\circ$. Figure 9 indicates that $\alpha = 0^\circ$ possesses the maximum absolute value of K_{III} at the left

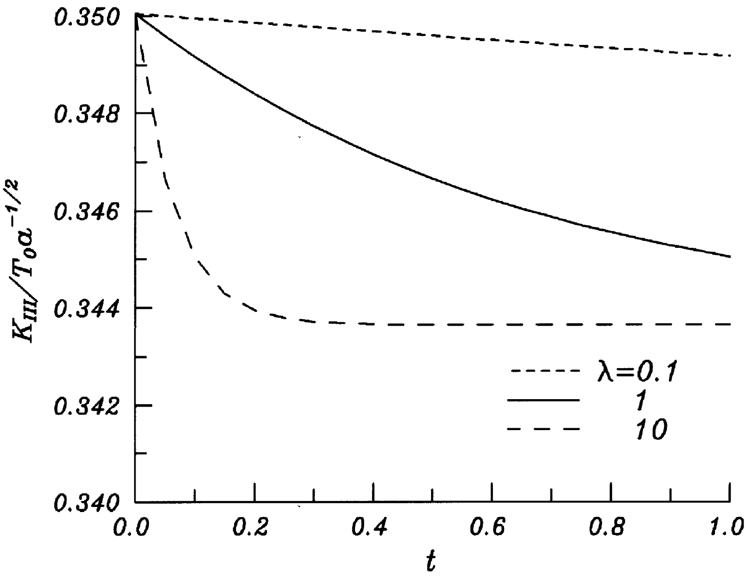

Fig. 6. Time-dependent stress intensity factor at crack tip-B for $\alpha = 0°$.

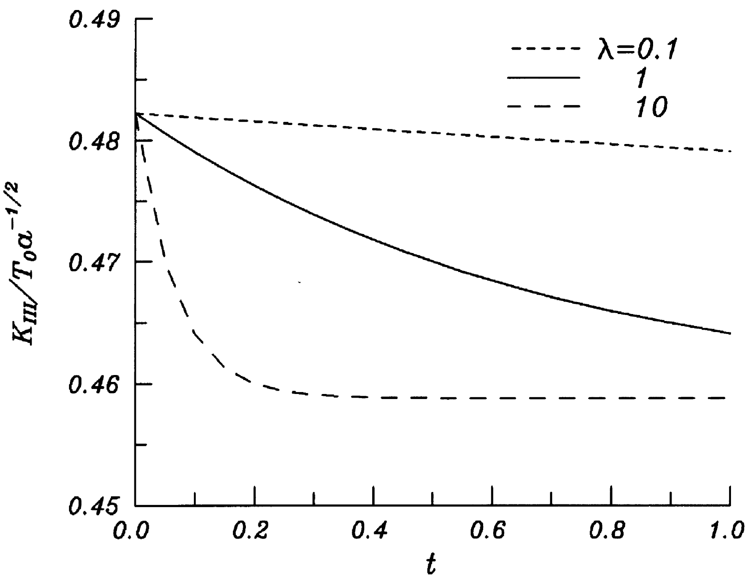

Fig. 7. Time-dependent stress intensity factor at crack tip-B for $\alpha = 45°$.

side crack tip, which is the negative value of the right side crack tip since the geometry is symmetric. In Figs 8 and 9, the variation of K_{III} is not evident with respect to the time change, since the relaxation time is relatively small ($\lambda = 1$). However, K_{III} varies as respected in Fig. 10 (crack tip-B) and Fig. 11 (crack tip-A) for the case of $\lambda = 10$. Note that $K_{\text{III}} = 0$ for each crack tip if the

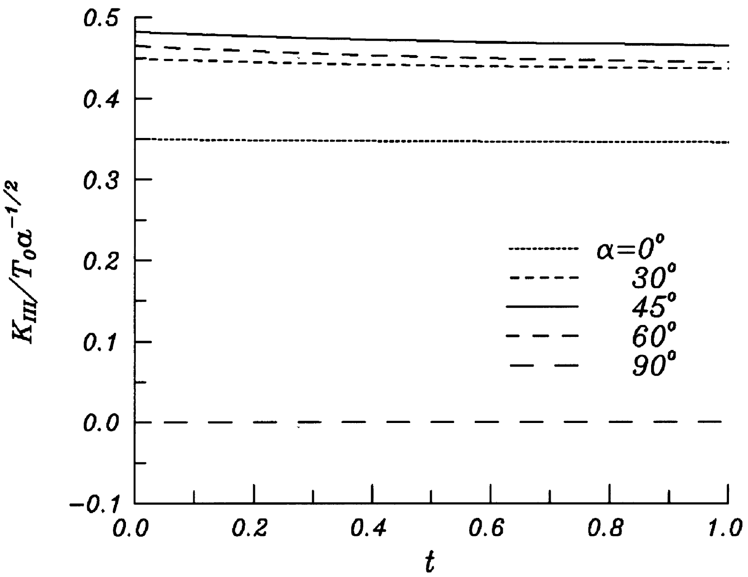

Fig. 8. Time-dependent stress intensity factor at crack tip-B for $\lambda = 1$.

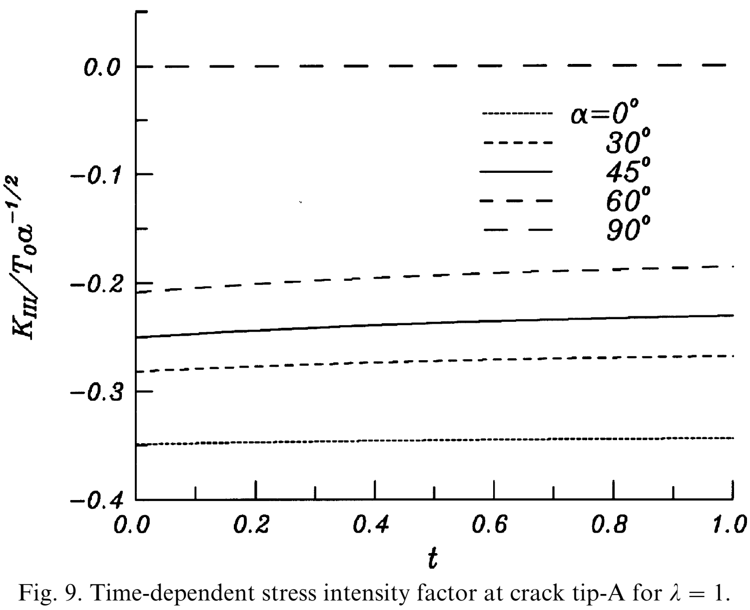

Fig. 9. Time-dependent stress intensity factor at crack tip-A for $\lambda = 1$.

crack is perpendicular to the load ($\alpha = 90^\circ$). Moreover, it must be emphasized that the absolute value of stress intensity factor decrease with time to approach the elastic value while the applied force remains constant, since the stiffness of the substrate is less than the crack layer. The time evolution of the stress intensity factor is affected by the orientation of crack as well as the relative

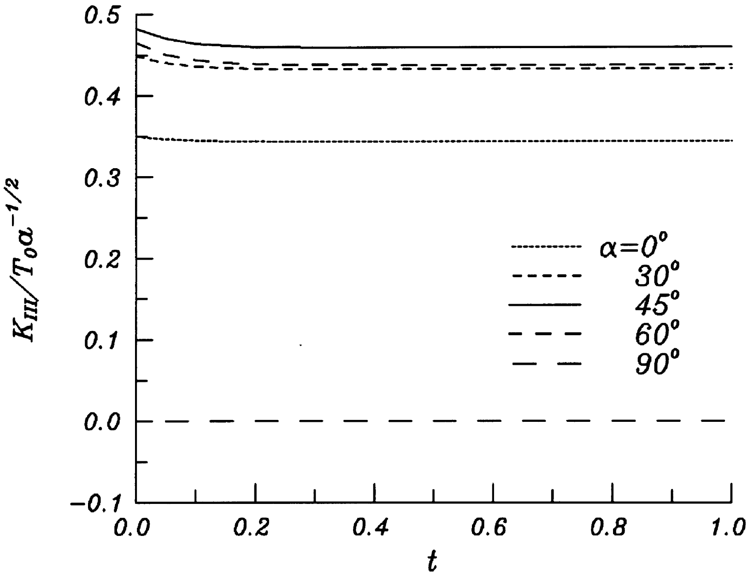

Fig. 10. Time-dependent stress intensity factor at crack tip-B for $\lambda = 10$.

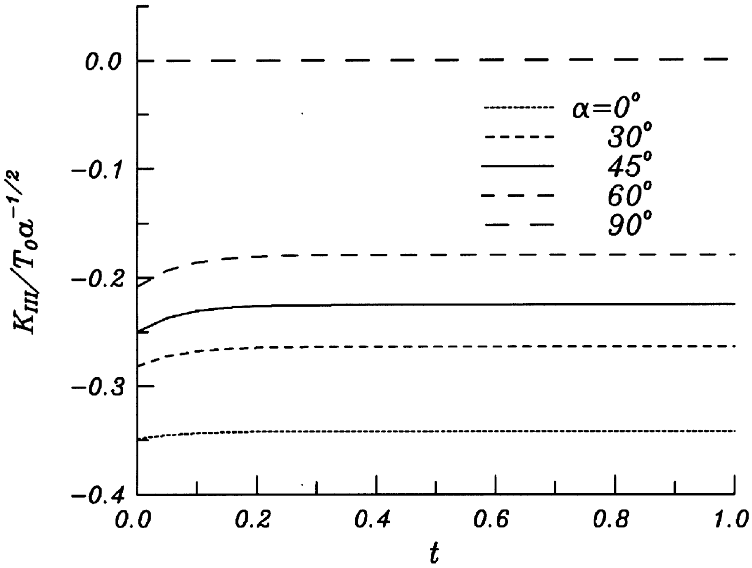

Fig. 11. Time-dependent stress intensity factor at crack tip-A for $\lambda = 10$.

strength of each medium. The skew-symmetry of K_{III} caused by the symmetry of geometry in the case of $\alpha = 0$ is still valid.

Figure 12 illustrates the numerical convergence of the given method with $\lambda = 10$, $\alpha = 0$. The general solution to the antiplane three-material media problem gives in eqns (31)–(33) is uniformly

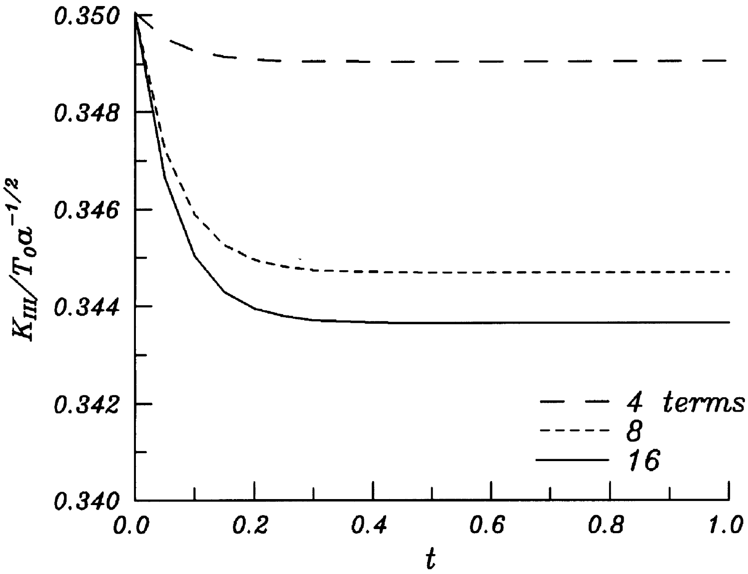

Fig. 12. Numerical convergence of time-dependent stress intensity factor at crack tip-B for $\lambda = 10$.

convergent on compact sets provided $|\alpha_1\alpha_2| < 1$ even for the case of $\alpha_i \pm 1$ (Honein et al., 1992). Figure 12 shows that the series solution has good convergence since the error between the first eight terms and the first sixteen is within 0.3 percent.

7. Conclusions

A general solution to a finite thickness cracked layer bonded to a viscoelastic substrate under antiplane shear is presented. Based on the Laplace transform and the analytical continuation theorem, a complex potential is formulated. The resulting singular integral equation with a logarithmic singular kernel is established from the resultant force across the crack surface. This leaves unknown dislocation function appearing in the singular integral equation which can then be solved numerically. Some typical examples are obtained by a Kelvin–Maxwell three parameters model of viscoelastic behavior. The result shows that, for long time, the viscoelastic solution will approach constant value, the elastic solution. It must be emphasized that the time-dependent stress intensity factor decreases while the applied force remains constant because the stiffness of the substrate is less than the crack layer. This shows that the time evolution of stress intensity factor is affected by the interaction of material strength of each layer as well as the relaxation time of viscoelastic medium. The results provides the reference to choose a suitable substrate to reduce the damage of the structure.

Acknowledgement

The author would like to thank the National Science Council, Republic of China, for their support through Grant No. NSC86-2212-E-129-001.

References

Atkinson, C., Chen, C.Y., 1996. The influence of layer thickness on the stress intensity factor crack of a lying in an elastic (viscoelastic) layer embedded in a different elastic (viscoelastic) medium (mode III analysis). Int. J. Engng. Sci. 34(6), 639–658.

Banks-Sills, L., Benveniste, Y., 1983. Steady interface crack propagation between two viscoelastic standard solids. Int. J. Fracture 21, 431–439.

Chao, C.K., Gao, B., 1997. A thin crack layer bonded to an elastic half-space under antiplane concentrated load. Int. J. Fracture, to appear.

Chen, Y.Z., Cheung, Y.K., 1990. New integral equation approach for the crack problem in elastic half-plane. Int. J. Fracture 46, 57–69.

Flügge, W., 1975. Viscoelasticity. Springer-Verlag, New York.

Honein, E., Honein, T., Herrmann, G., 1992. On two circular inclusions in harmonic problems. Quart. Appl. Math. 3, 479–499.

Irwin, G.R., 1957. Analysis of stresses and strains near the end of a crack transversing a plate. J. Appl. Mech. 24, 109–114.

Lekhnitskii, S.G., 1963. Theory of Elasticity of an Anisotropic Elastic Body. Holden-Day, San Francisco.

Saff, E.B., Snider, A.D., 1976. Fundamentals of Complex Analysis for Mathematics, Science, and Engineering. Prentice-Hall.

Schapery, R.A., 1984. Correspondence principles and a generalized J integral for large deformation and fracture analysis of viscoelastic media. Int. J. Fracture 25, 195–223.

Sills, L.B., Benveniste, Y., 1981. Steady state propagation of a mode III interface crack between dissimilar viscoelastic media. Int. J. Engng. Sci. 19, 1255–1268.